Through the Dust
Tracing Nebular Attenuation in Distant Galaxies

Ana Varo O'Ferrall (CAB - Madrid)

Collaborators: Irene Shivaei Javier Álvarez-Márquez JADES Collaboration

1. Introduction

Accurately characterizing dust attenuation in galaxies is key to uncovering their true intrinsic properties. While decades of research have established reliable methods at low redshift and Cosmic Noon (z < 3), the question remains: how does dust behave in the early universe? This project explores from the empirical point of view the dust attenuation curve for a sample of over 250 galaxies at 4 < z < 7 from the *JWST Advanced Deep Extragalactic Survey* (JADES), following the Calzetti et al. (2000) [1] method. This ongoing study aims to shed light on the understanding of dust in the first generations of galaxies.

2. Data and Sample

The sample consists of 257 galaxies from JADES[2] at 4 < z < 7, and is divided into bins according to dust content, traced by Balmer optical depth τ_b (from R1000 NIRSpec Balmer decrements Hα/Hβ), and sSFR (from NIRCam SED fitting):

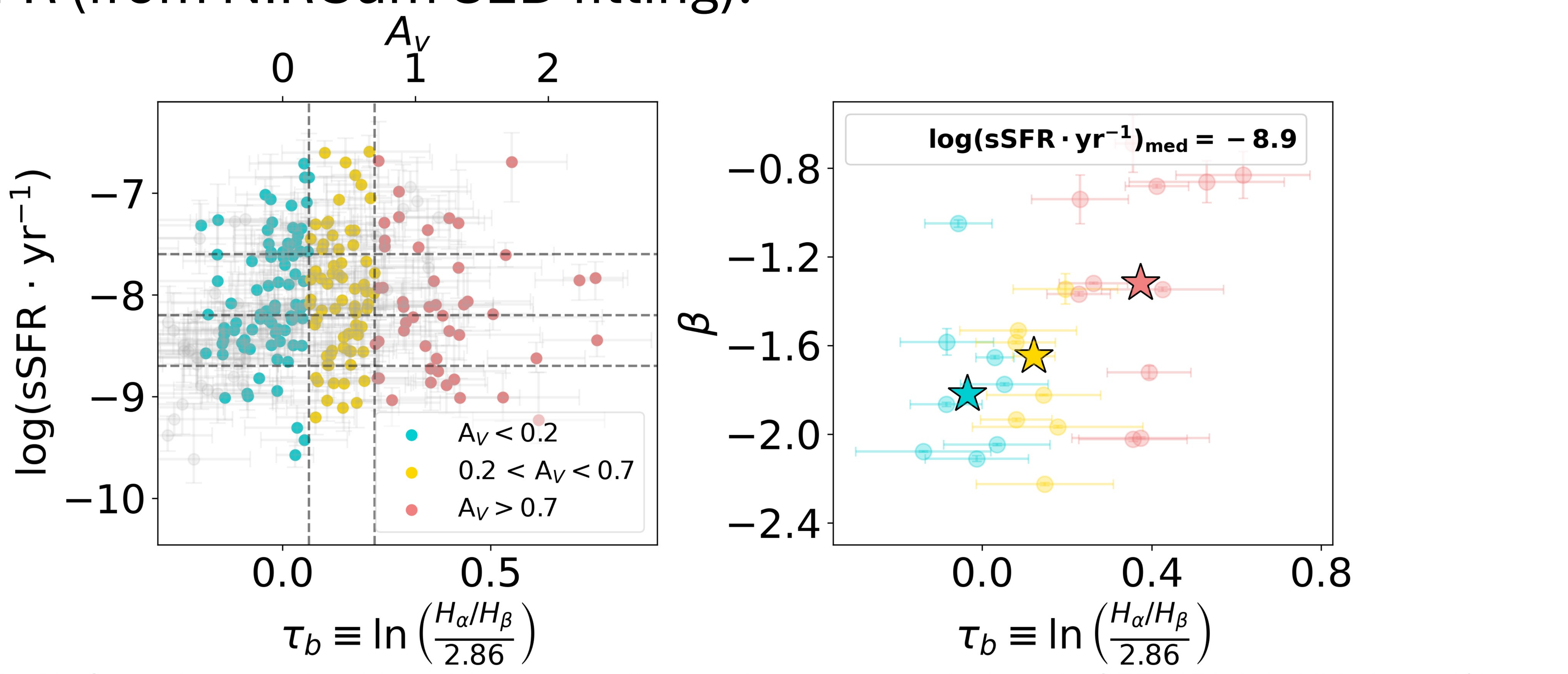

Figure 1. (*Left*): Sample organized into bins according to dust content (τ_b) and sSFR. (*Right*): UV slope (β) vs τ_b for the dust bins with median log(sSFR) = -8.9; the stars denote the median τ_b and sSFR values of the individual measures for each bin, showing a tight ascending correlation.

3. Methodology

3.1 UV Slope (β) to Cross-Match Dust Content

As a parallel check on the reliability of τ_b as a dust tracer, the UV continuum slope (β) is also derived from the best-fit photometric SED models. The slope becomes redder in dustier sources, allowing comparison with τ_b. Only those sSFR bins showing a clear increasing trend of τ_b vs β are selected (see Figure 1 (*Right*) as an example).

3.2 Average SEDs

To derive the attenuation curve for a given sSFR, an average SED is built for each dust bin by shifting all its models to rest-frame, normalizing at 5500 Å and averaging them after removing significant nebular emission line contributions.

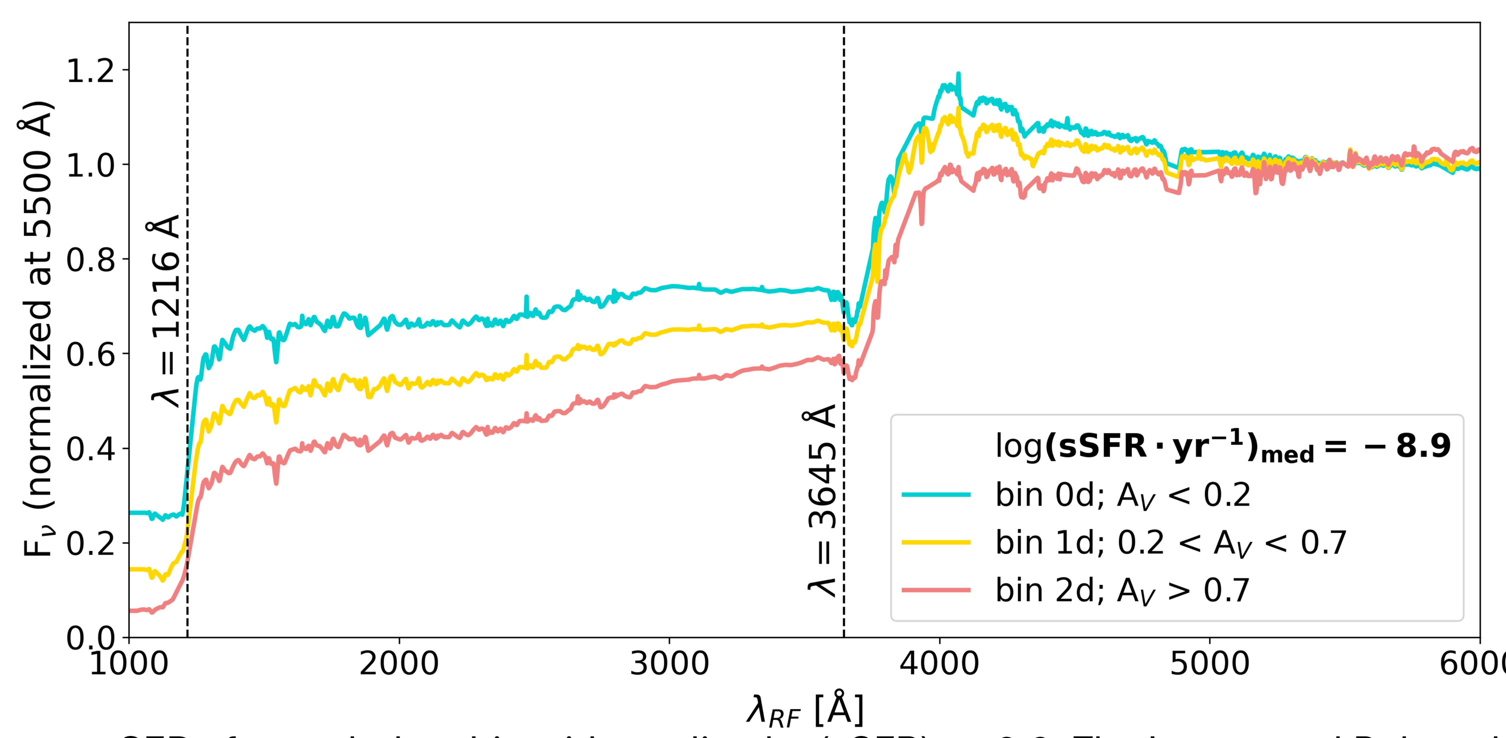

Figure 2. Average SEDs for each dust bin with median log(sSFR) = −8.9. The Lyman and Balmer breaks are both represented with a black dashed line. The SEDs present a descending vertical ordering with dust content, as expected from dust attenuation.

3.3 Selective (Q_i), Effective (Q_{eff}) and Total (k) Attenuation Curves

The selective curve of the *i-th* dust bin is defined as:

$$Q_i = \frac{-\ln\left(\frac{F_{\lambda,i}}{F_{\lambda,0}}\right)}{\tau_{b,i} - \tau_{b,0}} \quad (1)$$

where $F_{\lambda,i}$ and $F_{\lambda,0}$ are the average SEDs of the *i-th* and $\tau_b \sim 0$ bins, and $\tau_{b,i} - \tau_{b,0}$ the difference between their median Balmer depths. Q_{eff} is the average of all Q_is, and a second-order polynomial is fitted to it versus (1/λ) before proceeding. Finally, the total attenuation curve is:

$$k(\lambda) = fQ_{\rm eff} + R_V \quad (2)$$

With *f as a f*actor that adjusts the tilt and R_V as the extrapolated value of fQ_{eff}(2.85μm), where attenuation should be zero[3].

4. Results

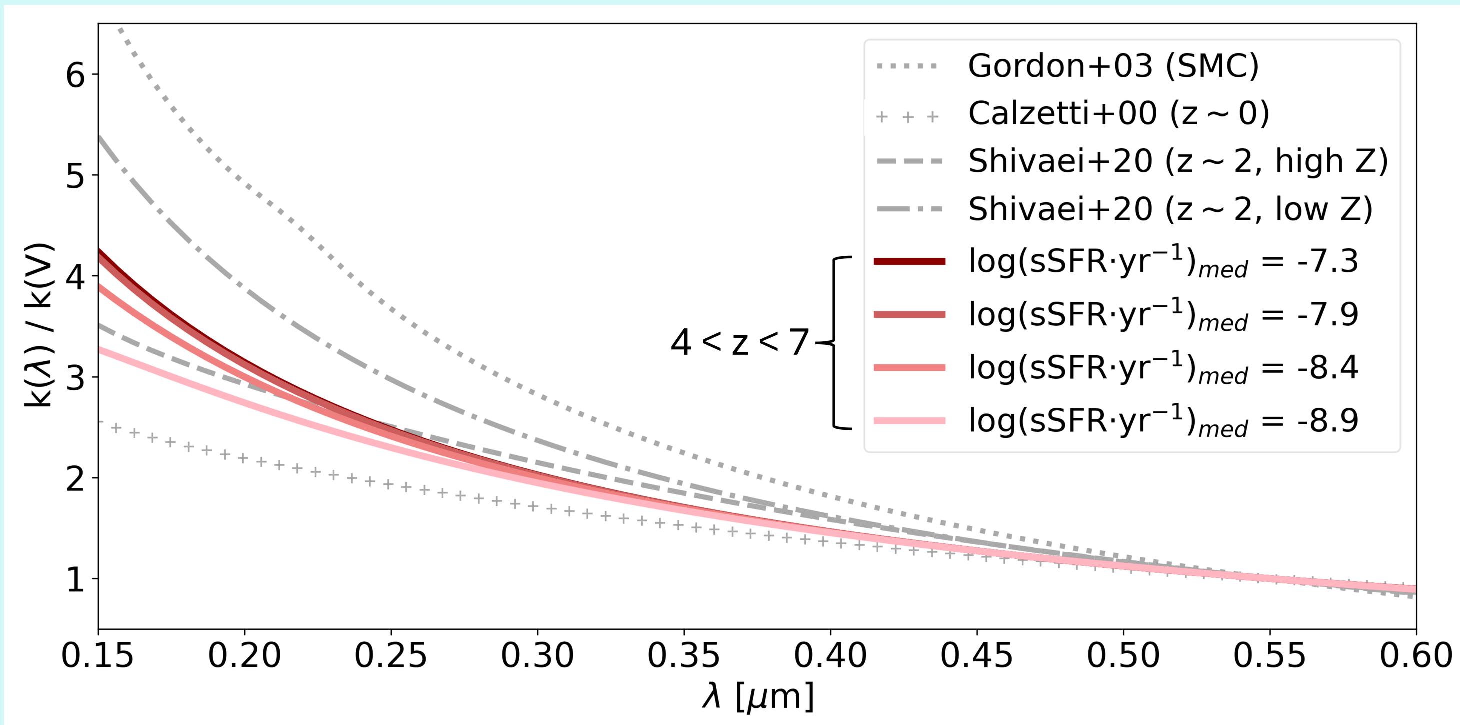

Figure 3. Total attenuation curves normalized at 5500 Å for the different sSFR bins (shades of red), and literature curves[1], [4], [5] (shades of gray) for comparison. The curves reveal a gradient from higher to lower sSFR towards grayer slopes.

★ The attenuation curve steepens with higher sSFR, likely due to stronger contribution of young stars affected by both birth-cloud and ISM dust that results in an optically thicker medium.[3], [6], [7]

★ Compared to the literature, low-sSFR curves align with older metal-rich systems, while high-sSFR curves approach younger metal-poor ones. This trend is consistent with the metallicity evolution implied by different sSFR regimes.[4]

★ Although a slope gradient with sSFR exists, the curves overlap within uncertainties (larger at higher sSFR). Improved SEDs may reduce errors, but if intrinsic, the curves will be indistinguishable.

5. Next Steps

★ **Refine the SED fitting models** to achieve a more accurate characterization of the attenuation curve and reduce uncertainties.

★ **Extend the analysis to galaxies with 3 < z < 4 from JADES** to investigate potential redshift evolution of the attenuation curve.

★ **Examine the dependence of the attenuation curve on additional galaxy properties** (e.g., stellar mass, metallicity, etc.).

AVO acknowledges fundings from the European Research Council (ERC) DistantDust (Grant No.101117541).

References (in order of appearance)

[1] *Calzetti, D. et al. 2000, ApJ, 533, 682*
[2] *Scholtz J. et al. 2025, p.arXiv:2510.01034*
[3] *Battisti, A. et al. 2017b, ApJ, 840, 109*
[4] *Shivaei, I. et al. 2020a, ApJ, 899, 117*
[5] *Gordon, K. D. et al. 2003, ApJ, 594, 279*
[6] *Salim S. et al. 2020, ARA&A, 58, 529*
[7] *Reddy, N. A. et al. 2015, ApJ, 806, 259*